THREE-DIMENSIONAL FLOW FIELD ANALYSIS IN RE-ENTRY PROBLEMS*

Gino Moretti
General Applied Science Labs.,Inc.
Westbury, New York

Abstract

A technique to compute three-dimensional steady supersonic flow fields, applying the method of characteristics, is described. The gas may be either a perfect one or real air in equilibrium. The technique has been worked out to provide solutions to practical problems and has been successfully applied to determine the whole flow field past winged hypersonic vehicles. In this paper, only unclassified sample computations are shown.

I. Introduction

The need for a detailed knowledge of the flow field past a three-dimensional body became imperative, since new problems like communication to and from the body in the re-entry phase arose. Oddly-shaped bodies and even axisymmetrical bodies at an angle of attack make axisymmetrical computations insufficient. Many attempts have been made to provide techniques for a numerical computation of three-dimensional flow fields but, as of our knowledge, none of them has been developed outside the range of an academic analysis. An historical survey can be found in (6).

Last year, the General Applied Science Labs.,Inc. was committed to furnish some complete computations of three-dimensional flow fields past re-entry bodies, and we faced the problem of providing a numerical tool in a relatively short time. We did not want to lose accuracy, but we wanted to maintain a very simple general scheme, to have a clear physical picture of the phenomenon. Simplicity also means storage space saving in the computer, as well as speed.

Our technique has been worked out from a basic idea: bodies for high altitude flights have a geometry which essentially is a combination of a blunted nose (often a portion of a sphere), a cone and a delta wing. For the time

*This work was sponsored by Aeronautical Systems Division, Air Force Sys.Command, USAF,Flt.Dyn.Lab., AF 33(616)7721.

being, the transonic region in the neighborhood of the stagnation point is assumed to be axisymmetrical; this assumption restricts the technique to bodies whose nose is axisymmetrical, and the reason for it is that we have available a program to compute axisymmetrical transonic regions (1). Nevertheless, steps are being made to extend this analysis to non-axisymmetrical blunted noses.

Let us assume then that a complete picture of the flow is available on a plane normal to the wind direction, where the flow is fully supersonic (no matter how close to 1 the local Mach number may be), but still axisymmetrical. Our task is to compute the supersonic flow behind that plane.

Now, as we pointed out before, the shape of the body downstream of the plane may partially be quasi-conical or may be that of a delta wing. In the vicinity of the quasi-conical part and of the leading portion of the wing, we consider the three-dimensional motion as close to an axisymmetrical flow field, whereas in the vicinity of the flat portion of the wing the three-dimensional motion is close to a two-dimensional flow field.

This does not mean that we want to linearize the equations of motion assuming that the motion itself is axisymmetrical or two-dimensional but for a small perturbation, whose higher powers will be neglected. On the contrary, we maintain the equations of the motion in their complete and exact form, but we will use a cartesian frame of reference where the flow tends to become two-dimensional and a cylindrical frame in the regions which have more resemblance to axisymmetrical fields. In either case, the method of characteristics will be applied to compute new points in cartesian or meridional planes which lie parallel to the wind, writing the exact equations to let the terms which express the influence of the cross flow appear as forcing terms. As far as the latter are small, as compared with the terms typical of a two-dimensional or axisymmetrical problem, the computation can be performed using a finite difference technique, that is with the same degree of accuracy which we use to find in a so-called exact numerical computation of a two-dimensional or axisymmetrical flow field.

II. Equations of motion

In what follows, we assume that the gas is inviscid and in equilibrium. Further extensions of the technique, under numerical checking at the present time, will not be discussed in this paper.

It is well known that the basic equations of motion are:

$$\rho(\bar{V}.\nabla)\bar{V} + \nabla p = 0 \tag{1}$$

$$\bar{V}.\nabla p + a^2\rho\nabla.\bar{V} = 0 \tag{2}$$

$$\bar{V}.\nabla(h + V^2/2) = 0 \tag{3}$$

$$\rho=\rho(p,h) \quad ; \quad a = a(p,h) \tag{4}$$

where

$\bar{V}$ = velocity vector

ρ = density

p = pressure

a = speed of sound

h = enthalpy.

Purposely, we do not specify the equation of state (4). If the range of pressure and enthalpy in the flow field is such that the perfect gas law holds, Eq.(4) has a very simple exponential form; but in many cases of practical interest the real gas must be taken into account. Fortunately, good tables and charts of the thermodynamical properties of real air are available (2 and 3). We worked out some fittings for density, temperature, speed of sound and entropy as functions of pressure and enthalpy, which cover a range of h from 0 to 500 RT_o (T_o being the absolute temperature at 0°C) and a range of p between .0001 and 1000 atm (4), with an accuracy better than 1%, which is widely sufficient for our purposes. The form of the fittings is such that the time involved in the computation of any thermodynamical parameter is comparable with a perfect gas computation, despite the wide range of validity of the formulæ.

The system of Eqs.(1) and (2) written in scalar form is different according to the frame of reference; but we already said that we can confine ourselves to cartesian and cylindrical frames.

We write now explicitly the equations for the cylindrical case, assuming r, θ, z as coordinates and calling u, v, w the corresponding radial, transverse and axial components of the velocity:

$$\rho(uu_r - v^2/r + vu_\theta/r + wu_z)+p_r = 0 \tag{5}$$

$$\rho(vv_\theta/r + wv_z + uv_r + uv/r)+p_\theta/r = 0 \tag{6}$$

$$\rho(ww_z + uw_r + vw_\theta/r) + p_z = 0 \tag{7}$$

$$up_r + vp_\theta/r + wp_z + a^2\rho(u/r + u_r + v_\theta/r + w_z) = 0 \tag{8}$$

The partial derivatives are indicated by subscripts. The cartesian equations are easily obtained by these, writing x instead of r, f_y instead of f_θ/r and dropping off every term which does not contain derivatives.

III. Reduction to a characteristic frame

A basic feature of a three-dimensional steady supersonic flow is the existence of characteristic surfaces. At any point, there exists a Mach cone, defined by:

$$\bar{V}.\bar{n} = a \tag{9}$$

where $\bar{n}$ is a unit vector normal to the cone. This cone is a characteristic surface related to that point. There is another characteristic line through any point, the streamline itself.

Let us choose an arbitrary line, not lying on characteristic loci, and consider the Mach cones and the streamlines at each point of it. The envelopes of the Mach cones are two characteristic surfaces, still defined by Eq. (9), and the stream surface is a third characteristic surface.

The equations of motion can be simplified if we take derivatives along the characteristic surfaces.

Let us choose the frame of reference in such a way that the angle between $\bar{V}$ and the (r,z)-plane is less than the Mach angle.

At a point **A**, the aforementioned arbitrary line can be chosen in order to get the equations in their most simple form. This is achieved if the line is an arc of a circle defined by: $r = \text{constant}$, $z = \text{constant}$ (Figure 1).

In this case, if α is the angle between $\bar{n}$ and $\bar{i}$ ($\bar{i},\bar{j}$ and $\bar{k}$ being defined by Fig. 1), we simply have

$$\bar{n} = \bar{i}\cos\alpha - \bar{k}\sin\alpha \tag{10}$$

$$\bar{V}.\bar{n} = u\cos\alpha - w\sin\alpha \tag{11}$$

and thus, Eq.(9) yields

$$u\cos\alpha - w\sin\alpha = a \tag{12}$$

Let us call bycharacteristics the intersections of the characteristic surface with the (r,z)-plane. Their slopes on the z-axis (Figure 2) are:

$$\lambda = \operatorname{tg}\alpha \tag{13}$$

and from Eq.(12) we obtain

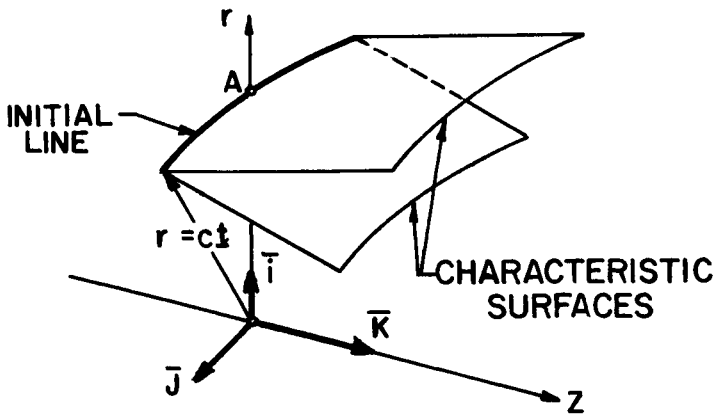

Fig. 1. Characteristic Surfaces.

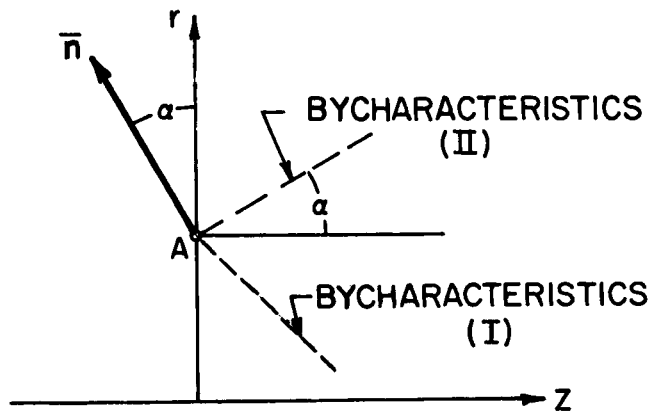

Fig. 2. Bycharacteristics.

$$\lambda^{I,II} = \frac{uw \mp a\sqrt{q^2 - a^2}}{w^2 - a^2} \tag{14}$$

where

$$q = \sqrt{u^2 + w^2} \tag{15}$$

is the modulus of the component of $\bar{V}$ in the (r,z)-plane.

As far as we are dealing with a small neighborhood of point A, we can assume that the slope of the intersection of the stream surfaces with the (r,z)-plane is given by

$$\lambda^{III} = \frac{u}{w} \tag{16}$$

As pointed out before, this is the third bycharacteristic.

The derivative of a function f along one of these directions, defined by some λ^k $(k = I, II, III)$ is

$$f_k = f_z + \lambda^k f_r \tag{17}$$

By suitable linear combinations of Eqs. (5),(7) and (8), the derivatives with respect to r and z will appear only combined together as in Eq.(17). Then if

$$\tau = u/w \tag{18}$$

and

$$\beta^2 = q^2/a^2 - 1 \tag{19}$$

we can write, instead of Eqs. (5),(7) and (8)

$$\rho w^2 \tau_I - \beta p_I = F^I \tag{20}$$

$$\rho w^2 \tau_{II} + \beta p_{II} = F^{II} \tag{21}$$

$$\rho(q^2)_{III} + 2p_{III} = F^{III} \tag{22}$$

whereas Eqs.(6) and (3) can be written

$$\rho w v_{III} = G \tag{23}$$

$$w\,(2h + q^2 + v^2)_{III} = H \tag{24}$$

Here the F^k-s, G and H are functions of the unknowns themselves and the derivatives of u, v, w and p with respect to θ. Obviously, for an axisymmetrical flow, Eq. (23) vanishes identically, F^{III} and H are also zero, whereas F^k is

$$F^k_{symm} = \rho u\,(u - \lambda^k w)/r \tag{25}$$

The right-hand side terms of Eqs. (20) to (24) minus F^k_{symm} are the forcing terms mentioned in the Introduction.

For the practical application of Eqs. (20) to (24), some remarks are of interest.

Obviously, their left hand sides lead to a technique similar to the method of characteristics for two-dimensional flow. The three-dimensional nature of the problem is concentrated in the right hand sides of the equations; in other words, in order to determine the rate of change of the physical quantities along the bycharacteristics, we need to know their rate of change in a transverse direction.

From a rigorous point of view, an interesting objection arises at this point. To compute derivatives with respect to θ, at a point A, we need information from point A itself and from a neighboring point A', which has the same r and z and a different θ. Now, if those derivatives are used to compute results at a point B downstream, both points A and A' must lie within the same Mach cone issued by point B in the upstream direction (which is the domain of dependence of point B for the hyperbolic system with which we are dealing). Otherwise, some disturbance or singularity which could happen to exist in a neighborhood of point A' would be taken into account in the computation of the physical values at B, whereas it is well known that no influence can be exerted on B from any point A' which lies outside its domain of influence.

This remark seems to complicate the computational technique very much, because for every point B the maximum admissible $\Delta\theta = |\theta_A - \theta_{A'}|$ should be determined, and this tends to decrease with increasing r. Nevertheless, as far as no discontinuities are present in the flow, there are no reasons for doubting about the soundness of the results, and the angle $\Delta\theta$ between A and A' is only limited by the obvious requirement that $\Delta f/\Delta\theta$ be a reasonable approximation to $\partial f/\partial\theta$.

IV. Boundary conditions on the body

The foregoing equations are used to compute points in the flow field, except those on the body and on the shock wave. At any point on the body, the condition of vanishing normal velocity must be applied:

$$\bar{V}.\bar{n} = \tau w\nu_1 + v\nu_2 + w\nu_3 = 0 \qquad (26)$$

(where ν_1, ν_2, and ν_3 are proportional to the components of any vector normal to the body surface).

Eq. (26) replaces Eq. (20) for any point on the body.

V. Shock wave equations

To compute a point on the shock wave, we assume, as usual, that the perturbation carried by the characteristic line which reaches the shock wave at a point P is so weak that no sizeable reflection takes place. Only the shock wave geometry will be changed, to satisfy the new conditions behind it at P.

Let $\bar{n}$ be a unit vector normal to the shock wave at P, V_n the normal component of the velocity, $\bar{V}_t$ its tangential component. We do not put any subscript to the physical parameters behind the shock wave, and indicate the free stream parameters with a subscript ∞. The following equations will apply:

$$p = p_\infty + (1 - \frac{\rho_\infty}{\rho}) V_{n\infty}^2 \rho_\infty \tag{27}$$

$$h = h_\infty + \frac{1}{2\rho_\infty}(\frac{\rho_\infty}{\rho} + 1)(p - p_\infty) \tag{28}$$

$$\bar{V}_{t\infty} = \bar{V}_t \tag{29}$$

The above equations are easily derived from the equations of conservation of mass, momentum and energy across the shock. In addition, we will use Eq.(21), which is valid along the characteristic which reaches the shock at P.

To complete the set of equations, let us examine Fig.3, where the unit vectors $\bar{i}, \bar{j}$ and $\bar{k}$ are respectively in the r, θ and z direction at P, and the z-axis is parallel to the wind. In the same figure, PN is the intersection of the shock wave with the meridional plane through P, PM is the intersection of the shock wave with the transverse plane $(\bar{i}, \bar{j})$ through P. Point M has the same z as P, and $\theta_M - \theta_P = \Delta\theta$. Let us call ϕ the angle between PN and the z-axis. The unit vector $\bar{n}$ is defined as

$$\bar{n} = \frac{(N-P) \times (M-P)}{|(N-P) \times (M-P)|} \tag{30}$$

but, with respect to the (r, θ, z) frame

$$N-P \equiv (\sin\phi,\ 0,\ \cos\phi) \tag{31}$$

$$M-P \equiv (r_M \cos\Delta\theta - r_P,\ r_M \sin\Delta\theta,\ 0) \tag{32}$$

Writing

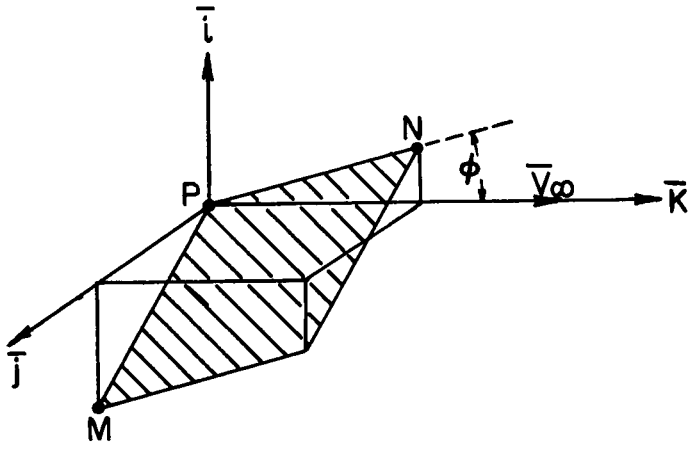

Fig. 3. Shock Wave

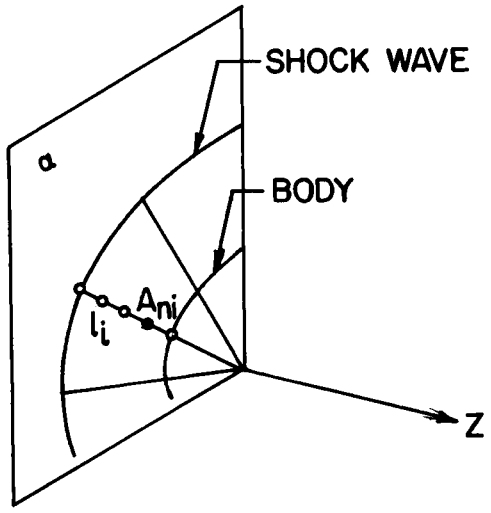

Fig. 4. Initial Points.

$$\xi = r_M \cos \Delta\theta - r_P$$
$$\eta = r_M \sin \Delta\theta \qquad (33)$$
$$R^2 = \eta^2 + \xi^2 \cos^2 \phi$$

we have

$$R\,\bar{n} \equiv (-\eta \cos \phi,\ \xi \cos \phi,\ \eta \sin \phi) \qquad (34)$$

Therefore

$$V_{n\infty} = V_\infty \frac{\eta}{R} \sin \phi \qquad (35)$$

and from Eq.(29) we obtain

$$v = V_{n\infty} \left(\frac{\rho_\infty}{\rho} - 1\right) \frac{\xi}{R} \cos \phi \qquad (36)$$

$$q^2 = V_{n\infty}^2 \left[\left(\frac{\rho_\infty}{\rho}\right)^2 - 1\right] + V_\infty^2 - v^2 \qquad (37)$$

$$\operatorname{tg} \phi = \frac{(V_\infty/w) - 1}{\tau} \qquad (38)$$

Eqs.(27),(28),(35),(36),(37),(38),(4) and (21) are the required set.

VI. Outline of the numerical technique

A simple numerical technique has been programmed on the basis of the foregoing equations. Let us assume that the flow is known on a plane α normal to the z-axis. The planes parallel to the x-axis and the z-axis in the cartesian frame, or the meridional planes in the cylindrical frame, intersect plane α along straight lines l_i (see Fig.4, where the cylindrical case is represented).

Saying that the flow is known on plane α, we mean that values of q^2, τ, v, p, h, u_θ, v_θ, w_θ and p_θ at several points A_{ni} on each line l_i are stored. The lines l_i are equidistant, and so are the points A_{ni}. Any l_i line contains the same number of points A_{ni}, the first of which is on the body, the last on the shock wave. In practical cases which have been worked out, the number of points on one l_i line did not exceed seven.

The machine is instructed to perform the same computation successively for all the l_i lines. The computation provides the values of λ^k, F^k, G, H at the points A_{ni}, determines the intersection C_{ni} of the two bycharacteris-

tics issued from any two points A_{ni} and $A_{n+1,i}$, and yields the values of τ and p at every point C_{ni}, using Eqs. (20) and (21). From the point C_{ni} a straight line whose slope is τ is issued backwards; its intersection A_{ni*} with the l_i line is determined and Eqs.(22),(23),and (24) are used to compute q^2, ρ, and h at C_{ni}. Linear interpolation is used between A_{ni} and $A_{n+1,i}$ to get the initial values at A_{ni*}. Then, the smallest value of $z_{Cni} - z_{Ani}$ is chosen to define another plane β parallel to α, on which we want to have the final output.

The intersections of β with the body and the shock wave are determined for all the meridional planes. At the intersection with the body the boundary condition is applied, forcing the entropy to be the same as on the intersection of plane α with the body. This is achieved choosing a tentative value of τ on the body, and iterating on τ, until the boundary condition (26) is satisfied.

At the intersections of β with the shock wave, the shock wave computation, outlined in Section V, is performed. Here again, a tentative value of $tg\,\phi$ is chosen, $V_{n\infty}$ is computed accordingly from Eq.(35), then p, h and ρ are determined from Eqs.(4),(27) and (28), τ is determined from Eq.(21), v and q^2 from Eqs.(36) and (37), and a new value of $tg\,\phi$ is obtained from Eq.(38). The procedure is iterated until a satisfactory value of $tg\,\phi$ is found.

Next, a double linear interpolation is performed, using values at points A_{ni} and C_{ni} to determine the values of q^2, τ, v, p and h at points E_{ni} which lie on the l_i lines of the plane β.

Polynomial fittings for u, v, w and p as functions of r are computed for each l_i line on the plane β and are used to compute the derivatives u_θ, v_θ, w_θ and p_θ.

At this stage, the values at points E_{ni} are stored on top of the values at points A_{ni}, and the plane β now plays the role of the plane α; therefore, the machine is ready to take another step forward in the z-direction.

It is seen that any step forward does not change either the number of meridional planes or the number of points A_{ni} on each of these planes. Therefore, the running time is the same at every step.

The use of the thermodynamical fitting mentioned in Section II and the simplicity of the formulae needed to compute points C_{ni} and the points on the body and the shock wave allow each step to be performed in a very short time, despite the number of linear interpolations and iterations involved.

For example, using 7 points on each l_i line and 10 meridional planes, twenty steps forward can be performed every

minute on an IBM 7090 computer. This estimate does not take printing time into account; of course, the latter depends on the amount of information desired to be printed out. If values of r, u, v, w, a, p, ρ, S, u_θ, v_θ, w_θ and p_θ are printed out at every step for all the points, the time is practically double; but for practical purposes these values are not needed every step; printing the outputs every tenth step will usually suffice.

VII. Remarks on the choice of the frame of reference

As we pointed out before, the frame of reference must be chosen according to the nature of the flow field. We actually applied this technique successfully to different bodies of quite complicated geometry; but, for the sake of illustration, let us consider a simple example.

A blunted nose delta wing is defined by a spherical nose of radius 1, two flat plates tangent to the sphere and two circular cylinders, also of radius 1, whose axes pass through the center of the sphere, are parallel to the flat plates and form an angle of 20° each with the centerline (Figure 5).

Let us confine ourselves to the 0° angle of attack case, in which the wind direction coincides with the centerline. In region 1 over the flat plate, the flow tends to become two-dimensional and the most suitable frame is a cartesian one, with its z-axis along the centerline and the x and y-axes as indicated in Figure 5.

In region 2 over the cylindrical leading edge region, the most suitable frame is a cylindrical one, with its origin located somewhere close to the OA line, its z-axis parallel to the centerline and its plane $\theta = 0$ parallel to the (x,z)-plane of the cartesian frame.

We worked out the problem at the beginning using a single cylindrical frame with its origin at O, but we found that, when the flat plate transverse dimension became important, the computation started losing accuracy. This agrees with our introductory remarks. The lack of accuracy was evidenced first where the angle between a l_i line and the body at a plane α was too far from 90° (for example, in the region of θ close to 45° in Figure 6).

Therefore, we decided to shift the origin of the cylindrical frame towards the OA line every once in a while, adding an extra cartesian plane in the region over the flat plate. The set of cartesian planes is schematically shown on Figure 7 (bold solid lines). The shadowed region is handled using cylindrical coordinates. The cross-flow deriva-

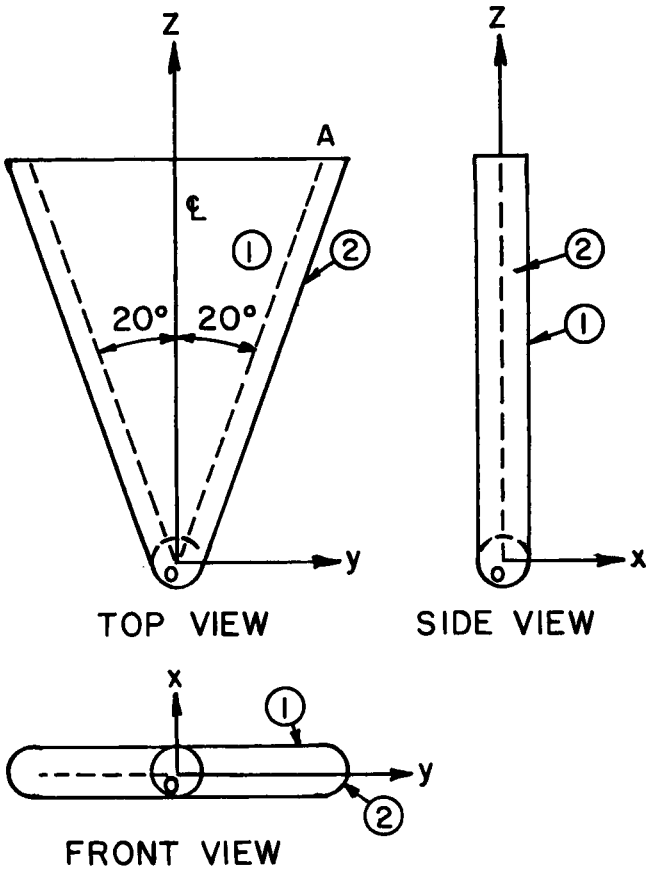

Fig. 5. Blunted Delta Wing Geometry.

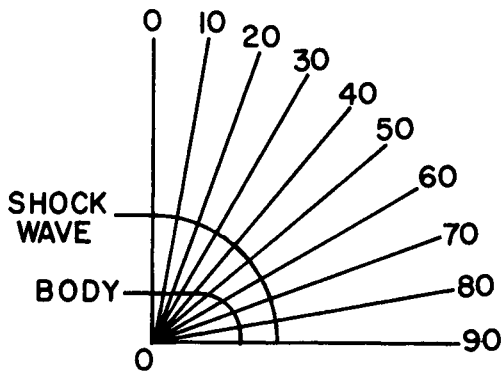

Fig. 6. Polar Coordinates in the α Plane

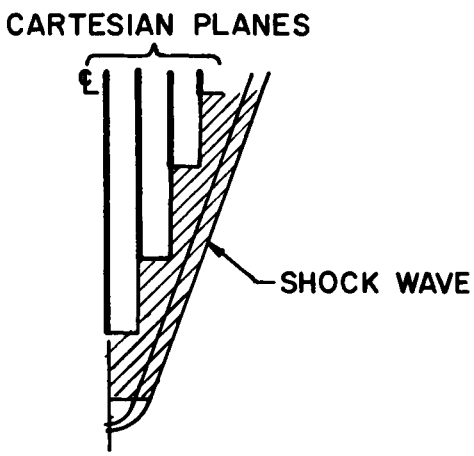

Fig. 7. Cartesian Planes and Polar Frame Region Seen From the Top of the Body.

tives are computed with a centered formula, using symmetry conditions on the symmetry planes and using one-side derivatives on the $\theta = 0$ plane in the cylindrical frame. In this way, information is fed from region 2 into region 1, which is physically sound, because in the matching region on the body the flow has a sizable cross-velocity directed towards the centerline.

As far as the shock wave is concerned, its shape does not depart too much from an axisymmetrical one. Therefore, its computation in a cartesian frame is not so clean as could be if computed in a cylindrical frame. Nevertheless, the results are still quite good and, in any event, slight inaccuracies introduced by the frame of reference on the shock wave propagate toward the body along characteristics, which means that they reach the body only at its rear.

A more sophisticated way of smoothing down these difficulties is based on the use of elliptic coordinates in any plane normal to the z-axis, instead of cartesian or polar coordinates.

The flow equations in this case become slightly more cumbersome, but they still maintain the same trend as in the aforementioned cases. On the contrary, the geometry of the elliptic coordinates can fairly well suit both the elongated cross-section of the body and the more circular shape of the shock wave.

A digital computer program using this particular system of reference has been worked out at GASL, but it has not yet been applied to any specific case.

VIII. Bodies at an angle of attack

For the body examined in the preceding Section, which has two planes of symmetry, the computation at zero angle of attack has to be made between the (x,z)-plane and the (y,z)-plane. For the same body at an angle of attack, the (y,z)-plane no longer is a plane of symmetry of the flow. In some cases the determination of the flow is requested only over a part of the body, for example the windward part. In principle, the computation should be made around the half of the body, starting and ending at the symmetry planes. Several reasons, particularly a need for saving machine time, suggested to confine the computation to the region of interest.

Actually, this can be done without introducing mistakes in the results. In fact, it has been found that in the region of any cross-section where the pressure reaches its maximum value, u and w also have stationary values and v changes its sign. In other words, these physical parameters

behave as at a symmetry plane. Now, if we take into account the region in which we are interested, from the symmetry plane to the stationary zone, plus another small portion of space behind it, and we compute one-sided derivatives at the last meridional plane, the stationary zone will appear automatically. The results at the last plane might not be very accurate, because part of the information has been neglected, but these slight errors will not penetrate beyond the stationary zone, thus leaving the computation valid in the region of interest.

IX. Results for the delta wing at zero angle of attack

Results of a computation performed for the body mentioned in Section VII are presented in a condensed graphical form in Figure 8. The computation has been made for a free stream Mach number equal to 8, and a free stream pressure equal to .00386 atm.

Fig. 8 shows a top view of the body, with lines of constant pressure on the body itself. It is worthy to observe that on the flat plate the differences between values of the pressure on two successive lines are one order of magnitude smaller than on the leading edge region. Therefore, little oscillations in the pressure close to the centerline should not be taken into account, because they are already beyond the accuracy to be expected in this coarse computation. It is evident that the machine tries to overrelax its results and keeps them oscillating around average values which are practically two-dimensional.

The shock wave is represented on the same figure as seen from the top. On the whole, its cross-section does not deviate too much from a circle. The typical overexpansion in the forward part of the body, which affects the shock wave shape, is detectable from the pressure lines and from the shape of the shock wave in the figure.

Experimental results obtained on the same body under similar circumstances (5) show a very good agreement with the computed values.

X. Another example: building up of a conical flow

Another interesting result has been obtained in relation with a computation which has been performed by Fowell (6), apparently to check some details of the technique that he is bringing to completion.

A cone of 20° semi-apex angle with a spherical nose is submerged in a flow at $M=8$, $\alpha=5°$. If the cone had a

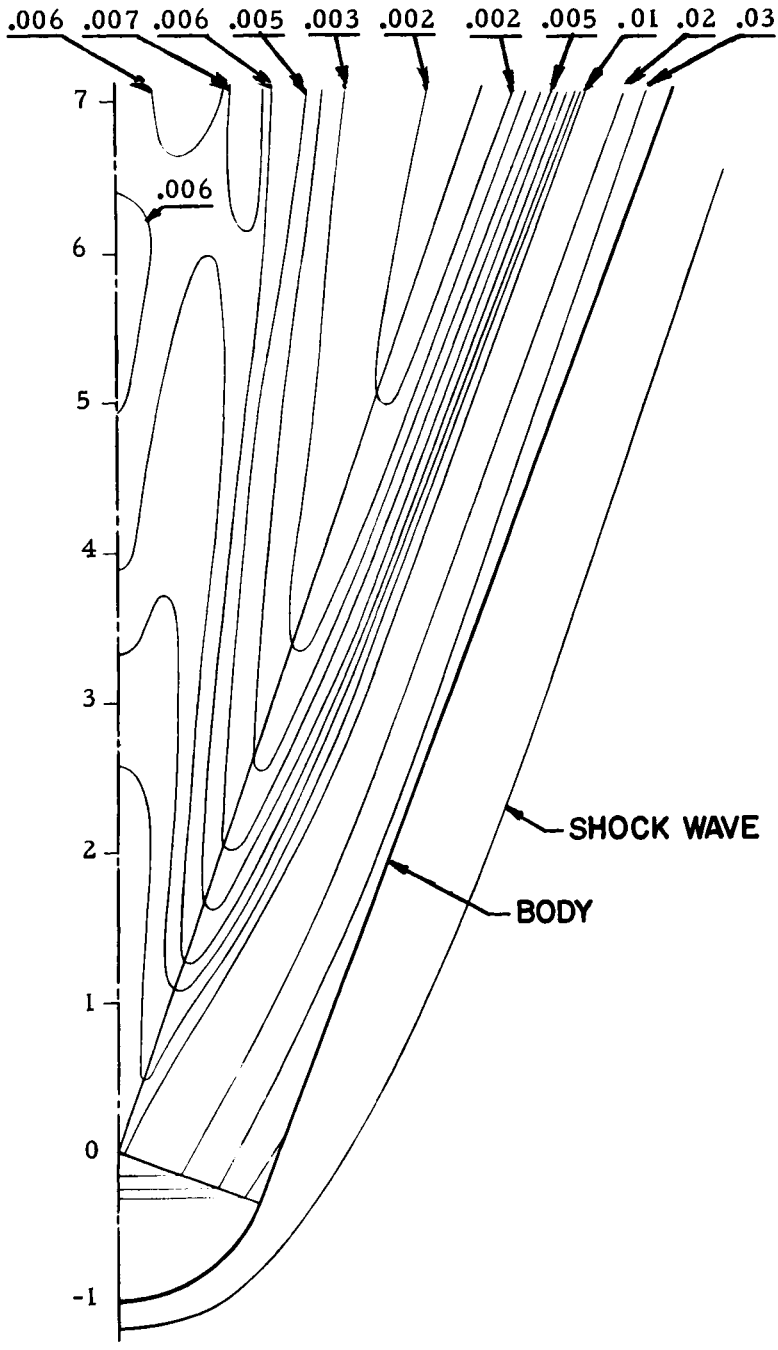

Fig. 8. Pressure Distribution on a Delta Wing (Atm).

pointed nose, the flow would be conical and, for such a small angle of attack, Kopal's tables (7) would be applicable to determine, for example, the cross distribution of pressure on the body. Nevertheless, even for a blunted cone, conical flow is established after a small number of nose radii in the axial direction.

We performed the three-dimensional computation of the flow around the blunted cone, using the same inputs as in the preceding example, a cylindrical frame of reference, and 19 meridional planes ten degrees apart from each other.

It took 204 steps to reach a distance of 10 radii from the center of the sphere, that is, 29.5 minutes on the IBM 7090.

The results appear graphically in Figs. 9, 10, and 11. Fig. 9 is a side view of the body and the shock wave. In Fig. 10 the pressure on the upper generatrix of the cone is plotted versus axial distance in nose radii. It is seen that a steady state is reached after 6 radii approximately. The matching of the numerical three-dimensional computation with either the conical flow theoretical data and the experimental results at M = 6 (8) is shown in Fig. 11.

In our opinion, this computation shows clearly the accuracy of our technique. It is not a simple check based on a set of initial data which are already consistent with a conical flow, but a true three-dimensional computation of a flow which is initially axisymmetrical but not conical, and asymptotically conical but no longer axisymmetrical.

XI. Conclusions

A technique has been described to compute supersonic three-dimensional steady fluid flows past any three-dimensional body at any angle of attack consistent with a fully supersonic flow.

All the significant kinetic and thermodynamical parameters can be determined, as well as the shape of the shock wave.

The fluid may be a perfect gas or real air in equilibrium.

The technique has been programmed for the IBM 7090 computer, and has been successfully applied to several different bodies. Further extensions are under way to analyze frozen and non-equilibrium flows.

Acknowledgments

The author is glad to acknowledge the valuable assistance given to him by Mr. E. Sanlorenzo in the preparation, analysis, and discussion of several practical applications, and by Mr. D. Magnus in the programming of the technique for the IBM machine.

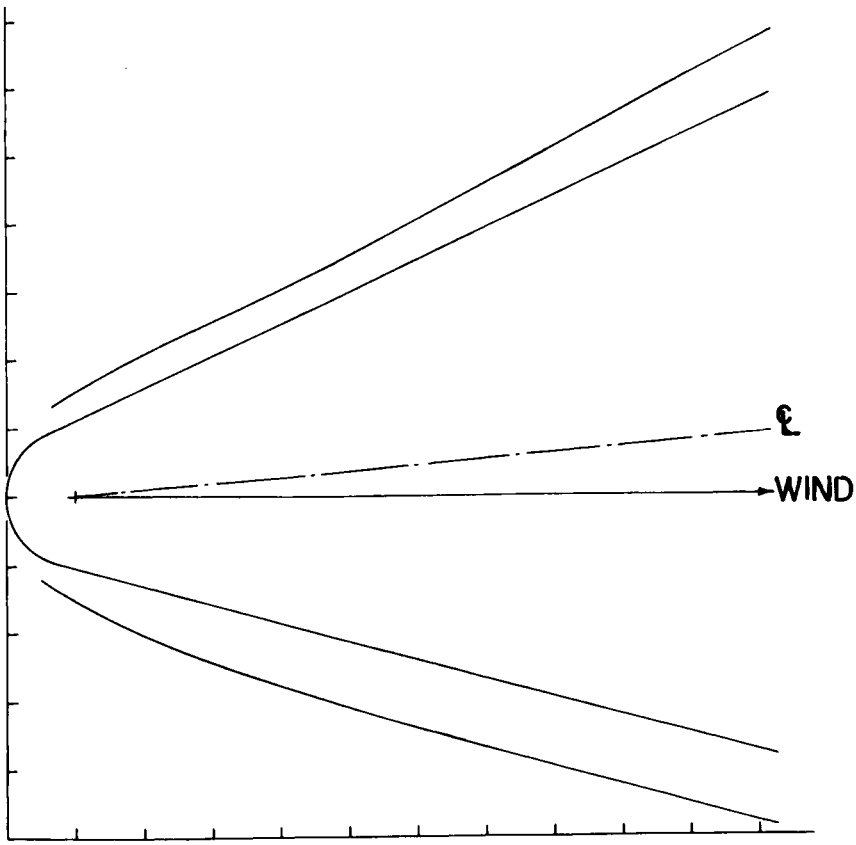

Fig. 9. Side View of a Blunted Yawed Cone and Its Shock Wave at M = 8.

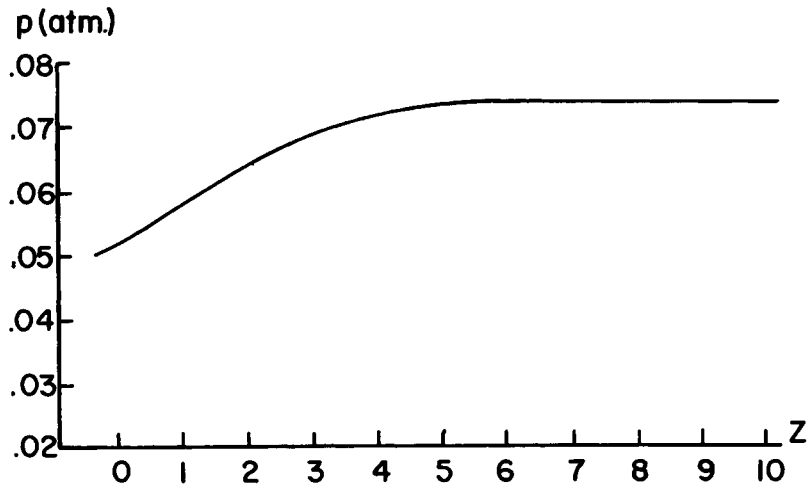

Fig. 10. Axial Pressure Distribution on the Windward Side of a Yawed Cone

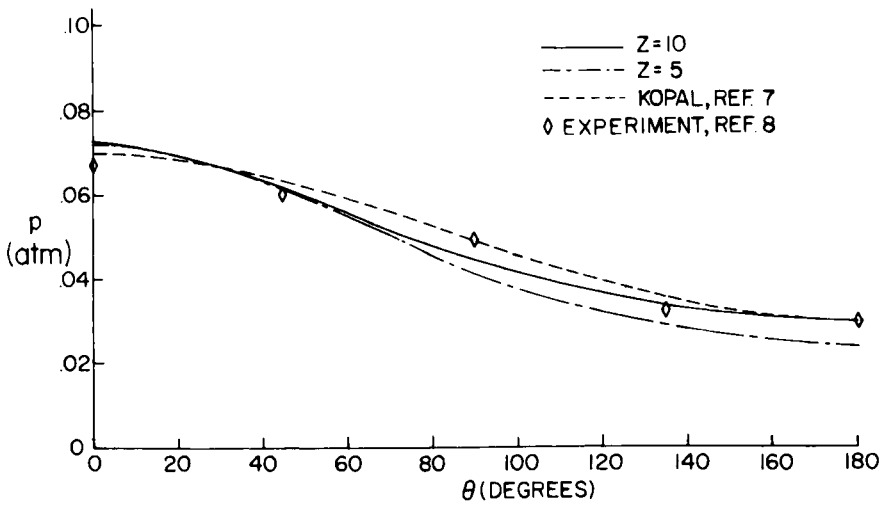

Fig. 11. Cross-Distribution of Pressure on a Yawed Cone.

References

1. Lieberman, E., "General Description of IBM 704 Computer Programs for Flow Field About Blunt-Nosed Bodies of Revolution in Hypersonic Flight", General Applied Science Labs., Techn. Report 134, Feb. 1960 (Rev. Mar. 1960).

2. Moeckel, W.E., and K.C. Weston, "Composition and Thermodynamic Properties of Air in Chemical Equilibrium", NACA TN 4265, April 1958.

3. Feldman, S., "Hypersonic Gas Dynamic Charts for Equilibrium Air", AVCO Research Laboratory, January 1957.

4. Moretti, G., "Analytical Expressions for a Speedy Computation of the Thermodynamical Properties of Air", General Applied Science Labs., Techn. Memo 39, November 1960.

5. Sanlorenzo, E.A., "Pressure Distribution on Blunt Delta Wings at Angle of Attack", General Applied Science Labs., Techn. Report 192, October 1960, Confidential Report, Title Unclassified.

6. Fowell, L.R., "Flow Field Analysis for Lifting Re-entry Configurations by the Method of Characteristics", Nat. IAS-ARS Joint Meeting, Los Angeles, California, June 1961, Paper No. 61-208-1902.

7. Kopal, Z., Tables of Supersonic Flow around Cones, MIT Dept. of Electrical Engineering, Center of Analysis, Techn. Rep. No. 1, Cambridge, Mass., 1947.

8. Zakkay, V., "Pressure and Laminar Heat Transfer Results in Three-dimensional Hypersonic Flow", WADC Techn. Note 58-182, September 1958.